JACS
JOURNAL OF THE AMERICAN CHEMICAL SOCIETY

Article

pubs.acs.org/JACS

Quantification of the Concentration of Aβ42 Propagons during the Lag Phase by an Amyloid Chain Reaction Assay

Paolo Arosio,[†] Risto Cukalevski,[§] Birgitta Frohm,[§] Tuomas P. J. Knowles,*[,†] and Sara Linse*[,§]

[†]Department of Chemistry, University of Cambridge, Lensfield Road, Cambridge, CB2 1EW, United Kingdom
[§]Department of Biochemistry and Structural Biology, Lund University, P. O. Box 124, SE221 00 Lund, Sweden

Supporting Information

ABSTRACT: The aggregation of the amyloid beta peptide, Aβ42, implicated in Alzheimer's disease, is characterized by a lag phase followed by a rapid growth phase. Conventional methods to study this reaction are not sensitive to events taking place early in the lag phase promoting the assumption that only monomeric or oligomeric species are present at early stages and that the lag time is defined by the primary nucleation rate only. Here we exploit the high sensitivity of chemical chain reactions to the reagent composition to develop an assay which improves by 2 orders of magnitude the detection limit of conventional bulk techniques and allows the concentration of fibrillar Aβ42 propagons to be detected and quantified even during the lag time. The method relies on the chain reaction multiplication of a small number of initial fibrils by secondary nucleation on the fibril surface in the presence of monomeric peptides, allowing the quantification of the number of initial propagons by comparing the multiplication reaction kinetics with controlled seeding data. The quantitative results of the chain reaction assay are confirmed by qualitative transmission electron microscopy analysis. The results demonstrate the nonlinearity of the aggregation process which involves both primary and secondary nucleation events even at the early stages of the reaction during the lag-phase.

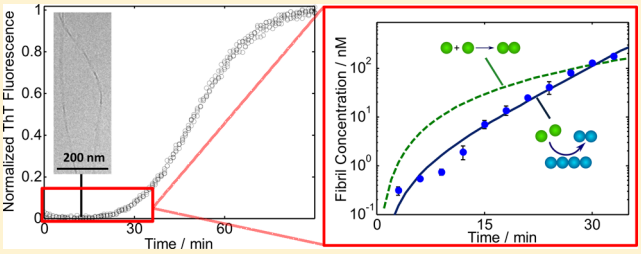

INTRODUCTION

The aggregation of soluble proteins and peptides into amyloid fibrils is increasingly associated with the progress of several neurodegenerative disorders, including Alzheimer's disease, a devastating dementia for which there is at present no cure.[1−4] Amyloid plaques of aggregated protein are found in the brains of affected individuals, although the plaques do not seem to be toxic per se.[5,6] One component of these aggregates is the 42-residue amyloid β peptide, Aβ42. Due to its potential implications in the disease, establishing the aggregation mechanism of Aβ42 is of great relevance for a molecular understanding of neurodegeneration. The high aggregation propensity of this peptide has presented significant challenges for experimental studies. After taking full control over Aβ42 monomer preparation and the inertness of the surfaces used in the kinetics experiment, we find highly reproducible kinetics of amyloid formation,[7,8] which are governed by multiple parallel microscopic processes in macroscopic samples.[9] This approach has allowed us to define the Aβ42 aggregation process in terms of underlying molecular events[7] in a similar manner to what has been possible in other self-assembling systems.[10−12] In the case of Aβ42, new aggregates are generated in three ways: primary nucleation of monomers in solution, secondary nucleation of monomers on fibril surface, and fibril breakage. Under quiescent conditions, the latter is a slow process, but surface-catalyzed secondary nucleation constitutes a fast positive feedback loop that creates Aβ42 oligomers that are toxic to neuronal cells.[7] The high reproducibility of our experimental setup allows us also to modify the aggregation conditions in a controlled manner and quantify their effect on kinetic profiles to derive mechanistic insights into the relative importance of the underlying microscopic steps of the process.

Kinetic growth curves for amyloid fibril formation starting from pure monomer display sigmoidal-like characteristics with a lag phase, a growth phase, and an equilibrium plateau. Although it is tempting to associate the lag phase and the growth phase exclusively to primary nucleation and elongation events, respectively, kinetic analysis has shown that none of these stages can be attributed to a single underlying microscopic event.[7−10] The processes of primary nucleation, elongation, and secondary nucleation events occur at all three stages albeit at different rates as governed by the rate constants and the concentration of the reacting species present at each point in time.[13] In order to obtain a comprehensive mechanistic picture of the aggregation process it is therefore crucial to characterize all the reacting species present at each time point. Typically, the aggregation process may be monitored by light scattering or spectroscopic techniques that distinguish aggregates from monomers, for example, CD spectroscopy reliant in the change to β-sheet rich aggregates[14] or thioflavin T (ThT) fluorescence that experiences an increased quantum yield when ThT binds to fibrils.[15] However, the resolution of these traditional

Received: August 23, 2013
Published: December 6, 2013

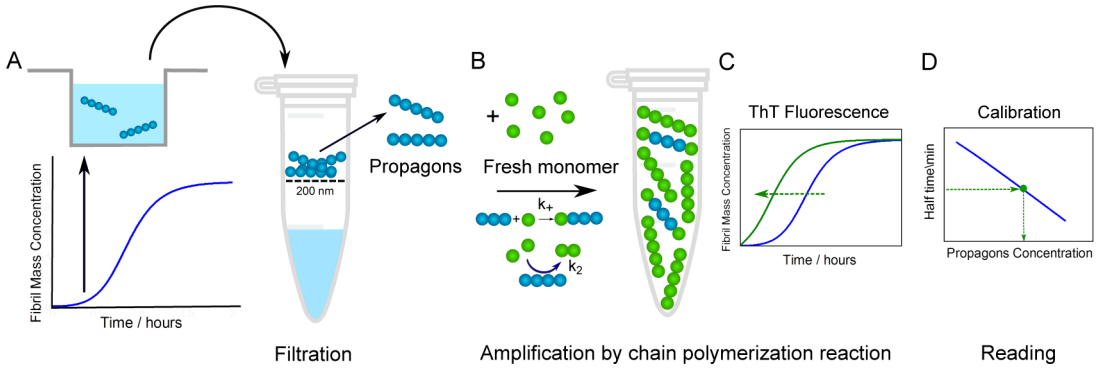

Figure 1. Principle of the chain reaction assay for the quantification of Aβ42 propagons during the lag phase. The propagons are isolated by filtrating sample aliquots (A) and supplemented with fresh monomeric solutions (B). The fibril amplification is monitored during time (C), and the original propagon concentration is quantified using a calibration curve based on reactions with controlled seed concentration (D).

techniques is insufficient to quantify the small concentration of aggregates formed during the lag phase.

In chemical chain reactions reactive species propagate rapidly by generating new reactive components. As a consequence, small perturbations of the reagent composition are rapidly propagated and are reflected in a significant modification of the global reaction rate, which can be accurately detected.

In this work, we exploit the high sensitivity of chemical chain reactions to the reagent composition to overcome the limitations of conventional biophysical techniques and design an experimental assay to quantify the concentration of fibrils formed during the lag phase of Aβ42 aggregation. Building on the theoretical mechanistic framework elucidated previously,[7] we induce the chain amplification reaction of a small amount of reactive preformed fibrils (seeds) by the addition of monomeric peptide. The technique is conceptually analogous to the polymerase chain reaction of DNA fragments[16] and to the protein misfolding cyclic amplification of prions,[17,18] which has been applied also for the quantification of fibrils in other protein systems.[19,20] In the case of Aβ42, the multiplication reaction amplifies the initial fibrillar mass by elongation and secondary nucleation events catalyzed by the accumulating fibril surface.[7,13] This multiplication rate can be accurately measured experimentally and rationalized by kinetic modeling analysis, allowing the quantification of the initial small number of fibrils.

RESULTS AND DISCUSSION

The principle of the assay is illustrated in Figure 1. The aggregation kinetics starting from pure monomeric Aβ42 are followed by ThT fluorescence. The fibrils formed at different time points during the lag phase are isolated by filtration and supplemented with fresh monomeric solutions to initiate the chain polymerization reaction. The amplification kinetics of the original fibrillar mass is monitored by ThT fluorescence, and the original concentration of propagons is quantified by comparison with a calibration curve obtained with controlled experiments initiated with a known concentration of seeds. We define a propagon as a seeding competent aggregate able to elongate and proliferate to form new fibrils, in analogy with the prion field.[21,22] It is worth specifying that we do not address in this work the structural features of the propagons and focus our attention on their quantification.

A fundamental information required by the assay is the *a priori* knowledge of the dependence of the chain polymerization reaction rate on the original propagon concentration. We obtained this calibration curve from seeded reactions with a known amount of seeds. The preformed fibrils were collected after 1.7 h incubation of a freshly prepared 4 μM Aβ42 monomer solution purified from inclusion bodies by ion exchange chromatography and repeated gel filtration steps[7,8,23] (Figure S1). The fibrils were then diluted with fresh monomer solution to yield samples with 4 μM Aβ42 monomer and no fibrils or fibrils at 15 concentrations ranging from 0.16 nM to 1.3 μM (counted as total monomer concentration in fibrils). Aggregation kinetics was monitored by recording ThT fluorescence as a function of time in a plate reader under quiescent condition at 37 °C. The lag time is found to decrease with seed concentration in a highly reproducible manner (Figure 2).

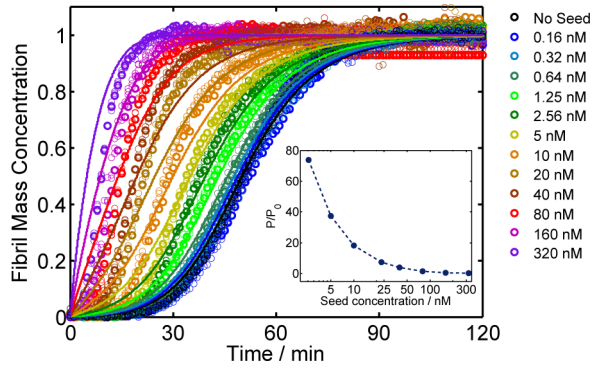

Figure 2. Aggregation kinetics for 4 μM Aβ42 in the absence (black) and presence of 0.16−320 nM preformed seeds (one color per concentration, four replicates of each). Continuous lines represent the integrated rate laws for Aβ42 using the previously determined rate constants. The insert shows the theoretical prediction of the multiplication factor of the initial number of propagons, P_0, by secondary nucleation events as a function of the initial propagon concentration.

The half time of aggregation ($t_{0.5}$) is defined as the point where the ThT fluorescence has reached 50% of the value at the post-transition plateau minus the pretransition baseline. In the presence of 0.16 or 0.32 nM seeds, $t_{0.5}$ is within error limits the same as when starting with pure monomer (Figure 3). Between 0.64 and 320 nM seeds (corresponding to 0.016−8% of the free monomer), $t_{0.5}$ is found to decay linearly with the logarithm of the seed concentration:

$$t_{0.5}/t_0 = 43.3 + 14.6 \log(C_{seed}/C_0) \quad (1)$$

dx.doi.org/10.1021/ja408765u | J. Am. Chem. Soc. 2014, 136, 219−225

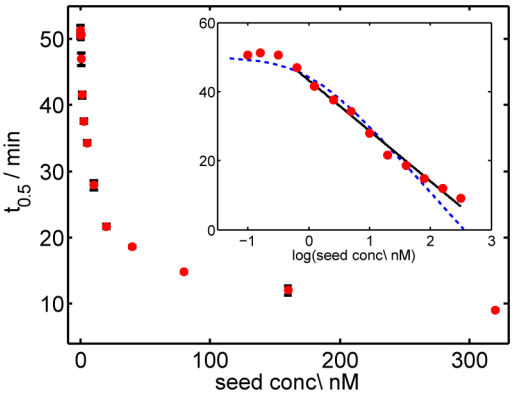

Figure 3. Calibration of the dependence of the half time for aggregation of 4 μM Aβ42 on the concentration of preformed seeds added at time zero, average, and standard deviation over four replicates from Figure 2. The inset shows the same data plotted versus the logarithm of seed concentration with a linear fit to data between log(0.64) and log(320) (continuous black line) and with the simulation predicted using the previously determined rate constants (blue dot line).

where t_0 and C_0 represent a reference time and a reference concentration equal to 1 min and 1 nM, respectively.

At higher seed concentration, the apparent acceleration of the reaction begins to level off as the high seeding regime is reached where elongation tends to dominate. The experimental data are supplemented with theoretical predictions of the seeding effect, using recently determined values of the rate constants for all microscopic steps in the Aβ42 aggregation mechanism[7] and incorporation of different amounts of preformed seeds at zero time.[24,25] The calculations predict a range of seed concentrations (5−310 nM) at which the half time for aggregation decreases in a roughly linear fashion with the logarithm of the seed concentration at constant monomer concentration, in good agreement with the experiments (Figures 3 and S6). In addition, the kinetic theory predicts a slope in the linear regime equal to 19.3 min and a half time for the unseeded experiment equal to 50 min, which are also in excellent agreement with the values measured experimentally (equal to 14.6 and 50.1 min, respectively, see SI). The simulated overall kinetic reaction profiles are shown in Figure 2. It is remarkable that the system performs almost exactly as predicted from the theory based on the previously determined rate constants. It is interesting to note that according to the theoretical predictions, the autocatalytic effect related to secondary nucleation processes decreases with increasing seed concentration (see Figures 2 and S5), since the fibrils preferentially sequester soluble monomers by fast elongation. This observation predicts that the oligomer concentration produced by nucleation pathways is lower in solutions seeded with mature fibrils than in unseeded solutions. However, the maximum rate of oligomer production by secondary nucleation is higher and peaks at earlier time the higher the seed concentration (Figure S5c).

After determining the effect of the seed concentration on the aggregation kinetics, we performed the "trap-and-seed" experiments to quantify the propagon concentration during the lag phase of a nonseeded reaction (Figure 1). Freshly prepared 4 μM Aβ42 monomer solution was incubated at 37 °C under quiescent condition for 0−33 min. Samples were taken at 3 min intervals (Figure 4A) and separated by centrifugation through a

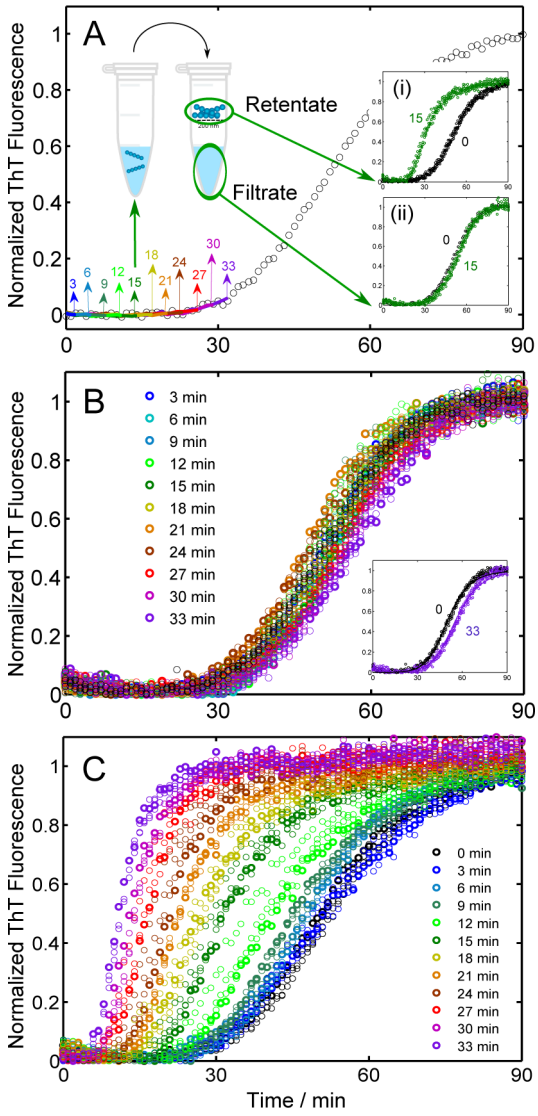

Figure 4. Trap-and-seed experiment. (A) A nonseeded Aβ42 aggregation reaction started with 4 μM monomer. Samples were taken during the lag phase at 11 time points as indicated by separate colors and filtered through a 200 nm filter, as illustrated for one representative sample. The dark circles (○) show the average of four samples that remained untouched up to 1.5 h. (B) Each filtrate was moved to a new plate, and its aggregation monitored by ThT fluorescence. Four replicates are shown for each filtration time point. (C) Each retentate was added to solutions of fresh 4 μM monomer, and the aggregation monitored by ThT fluorescence. Four replicates are shown for each trapping time. The whole experiment was repeated twice with very similar results.

200 nm filter. The propagons contained in the retentates were supplemented with fresh monomeric solution to initiate the chain polymerization reaction assay, while the filtrates were used in separate control aggregation kinetics experiments.

The filtrates from samples collected between zero and 27 min show similar kinetics, implying that close to 100% of the sample remains monomeric until the end of the lag phase (Figures 4B and S2). A small delay is seen for the sample filtrated at 33 min, where the ThT signal has started to rise. This reflects the high sensitivity of the aggregation kinetics to monomer concentration.[7,8] A few % reduction in the monomer

dx.doi.org/10.1021/ja408765u | J. Am. Chem. Soc. 2014, 136, 219−225

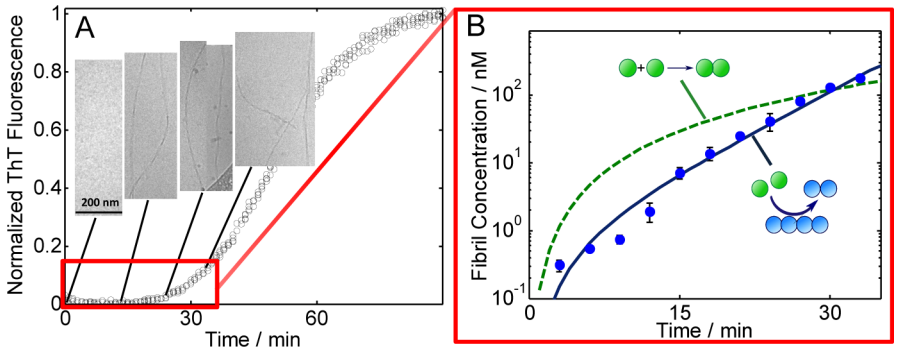

Figure 5. (A) Kinetics of a nonseeded Aβ42 reaction started with 4 μM monomer. The insets show cryo-TEM pictures of samples taken at the time points indicated by the black lines from the respective panels. (B) Fibril concentration as a function of time during the lag time. $t_{0.5}$ was obtained from the trap-and-seed data (Figure 4), and C_{fibril} estimated using eq 2. The average and standard deviation are based on the four replicates at each trapping time. The continuous blue line is the proper fitting of the cosh function representative of secondary nucleation events, while the green dot line is the poor fitting of the t^2 function characteristic of primary nucleation events.

concentration at the end of the lag phase causes a small but noticeable delay of aggregation (inset in Figure 4B).

The retentate from each filter was supplemented with fresh 4 μM Aβ42 monomer and aggregation kinetics studied by ThT fluorescence (Figure 4C). The monomer solution was added into the filter unit and then transferred into a 96-well plate to ensure complete recovery of the trapped propagons. In Figure 4C we show four replicates for each trapping time. It is interesting to note that the excellent reproducibility of the kinetic experiments (see also Figure S2C) is a robust indirect proof of the accuracy of the fibril recovery during the filtration step. In fact, because of the high sensitivity of the reaction to the initial seed concentration, even a small difference in the initial propagon concentration due to incomplete recovery would be reflected in a significant difference in the aggregation kinetics. The kinetics with retentates collected at 0 and 3 min do not differ from the unseeded aggregation kinetics beyond error limits. Retentates collected after 6 min and onward are found to cause a reproducible decrease in $t_{0.5}$, which is more pronounced the later the retentate is collected. Thus, the lag time decreases in a systematic manner with the time spent before collecting the retentate, corresponding to an increasing concentration of trapped propagons which serve as seeds for monomer depletion. Already after 6 min of a nonseeded reaction, the fibrils have reached high enough concentration to give a measurable effect in the trap-and-seed experiment. From the quantitative comparison of the reaction kinetics observed in the trap-and-seed experiment (Figure 4C) with the results of the controlled seeding experiment (Figures 2 and 3), we measured the concentration of fibrils formed at very early stages during the lag phase, which is not high enough for detection by ThT until the end of the lag phase.

The half times, $t_{0.5}$, of aggregation reactions that were seeded with retentates from 0 to 33 min, were used to estimate the propagon concentration as a function of time during the nonseeded reaction using the inverse of the calibration line in Figure 3.

$$\log(C_{\text{fibril}}/C_0) = (t_{0.5}/t_0 - 43.3)/14.6 \quad (2)$$

In Figure 5 it can be appreciated how this strategy improves the detection resolution by 2 orders of magnitude over bulk ThT fluorescence assays and provides accurate quantification of the fibril concentration in the nanomolar regime, which is not accessible by conventional experiments.

The fibril concentration during the lag phase of the nonseeded reaction (Figure 5) is well-fitted by the functional form:

$$C_{\text{fibril}}/C_0 = A[\cosh(\kappa t) - 1] \quad (3)$$

with $A = 1$ and $k = 0.003$ s^{-1}. This function describes in a closed expression the macroscopic self-assembly process of several systems in the presence of both primary and secondary pathways.[25,26] The parameter $A \sim k_n/k_2$ is related to the nucleation of new fibrils and in particular to the relative contributions of primary (k_n) over secondary (k_2) nucleation events, while the coefficient $\kappa \sim (k_+k_2)^{1/2}$ is an effective polymerization rate constant which reflects the multiplication and growth rates of fibrils due to elongation (k_+) and secondary nucleation (k_2) processes. The values of A and κ fitted to the experimental data in Figure 5 correspond to a set of combinations of microscopic kinetic constants equal to $k_+k_2 = 7 \times 10^{10}$ s^{-2} M^{-3} and $k_n/k_2 = 1 \times 10^{-9}$ M (see SI), which are in good agreement with the values previously obtained by the analysis of nonseeded kinetics of Aβ42 fibril formation during the overall time course of the process,[7] $k_+k_2 = 3 \times 10^{10}$ s^{-2} M^{-3} and $k_n/k_2 = 3 \times 10^{-8}$ M, thus confirming the robustness of our experimental system and theoretical analysis. It is worth noting that for a system characterized only by primary nucleation and elongation the time evolution of the fibril concentration in the early stages is expected to exhibit a quadratic dependence on time.[12] In Figure 5B we show how the best fitting of the quadratic (C_{fibril} / $C_0 = Bt^2$) function to the experimental data clearly fails to describe the experimental time dependence of the fibril concentration, therefore confirming the presence of secondary nucleation events.

The evaluated fibril concentration at 33 min is in good agreement with the concentration of converted monomer estimated by the kinetic experiment with the retentate (see SI and inset in Figure 4B), indicating that most of the converted monomer is present in the form of fibrils.

This quantitative analysis is complemented with cryogenic (cryo-TEM) and transmission electron microscopy (TEM) of samples taken from an ongoing reaction at zero time, during the lag phase, close to $t_{0.5}$ and at the equilibrium plateau (Figures 5A and S3), which confirm the absence of fibrils at time zero and the presence of fibrils during the lag phase.[7,27]

The results of the current study are a clear manifestation of the nonlinear sequence of events leading from pure Aβ42 monomer to an equilibrium solution dominated by fibrillar

dx.doi.org/10.1021/ja408765u | J. Am. Chem. Soc. 2014, 136, 219−225

aggregates (Figure 6).[7] Initially, at zero time, when there are only monomers in solution, the only process that can lead to

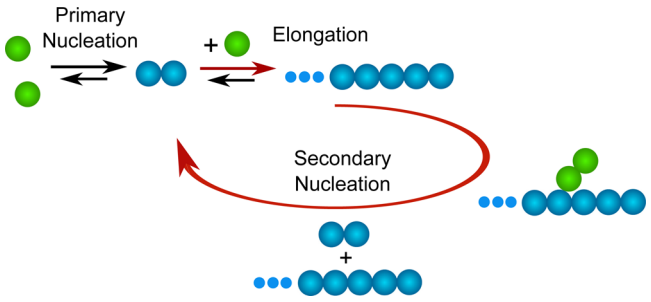

Figure 6. Aβ42 aggregation mechanism with secondary nucleation on the surface of fibrils providing an autocatalytic feedback loop (red).

formation of new aggregates is primary nucleation. This is an intrinsically slow process. Some primary nuclei dissociate into monomers, but some grow further by the addition of monomers. Therefore, some fibrils appear already during the very early part of the lag phase. These fibrils present a catalytic surface for secondary nucleation of monomers. This process has a higher rate than primary nucleation. Again, some nuclei may dissociate into monomers, but some grow to form new fibrils. This process generates more catalytic surface and a positive feedback loop for the aggregation process (Figure 6), resulting in the autocatalytic kinetics observed experimentally. The quantitative mechanistic description of the aggregation process is supported by the trap-and-seed experiment, which allows accurate measurements of the fibril concentration in the nanomolar range already at 6 min into the lag phase, long before the signal has increased above the noise in the ThT measurement.

The secondary nucleation reaction is the process giving rise to the majority of toxic species,[7] and insights into this process may shed light on the molecular origins of Alzheimer's disease. Moreover, heterogeneous secondary nucleation pathways are increasingly recognized in a large number of protein aggregating systems associated with other diseases.[10,25,28−33] It is therefore expected that the technique described in this work has general validity and could be applied to many other proteins. The determination of the molecular aggregation mechanism of Aβ42[7] put us in the position to apply in a fully quantitative way the chain reaction assay to this challenging peptide. Analogous mechanistic studies on other proteins will open the possibility to apply the chain reaction assay also to other systems.

CONCLUSIONS

In conclusion, we describe a highly sensitive assay to quantify the concentration of fibrils during the lag phase of Aβ42 kinetics by inducing a chain reaction multiplication of an initial number of propagons. Conventional techniques do not provide sufficient resolution to detect the presence of fibrils until the end of the lag phase. By contrast, the trap-and-seed experiments presented here improve by 2 orders of magnitude the detection sensitivity relative to traditional assays, thereby allowing accurate quantification in the nanomolar regime. The results show the nonlinear nature of Aβ42 aggregation process in which the fibrils provide a catalytic surface for secondary nucleation events which dominate over the elongation and primary nucleation processes even during the early stages of the reaction.

EXPERIMENTAL SECTION

Materials. The Aβ42(M1−42) peptide (MDAEFRHDSGYEVHHQKLVFFAEDVGSNKGAIIGLMVGGVVIA), here called Aβ42, was expressed in *Escherichia coli* from a synthetic gene and purified as described in Walsh et al., 2009,[23] except that size exclusion with spin filters was replaced by gel filtration. In short, the purification procedure involved sonication of *E. coli* cells, dissolution of inclusion bodies in 8 M urea, ion exchange in batch mode on DEAE cellulose resin, lyophilization, and gel filtration on a 3.4 × 200 cm gel filtration column at 4 °C. The purified peptide was frozen as identical 3 mL aliquots and lyophilized. All chemicals were of analytical grade.

Preparation of Samples for Kinetic Experiments. For kinetic experiments, aliquots of purified Aβ42 were dissolved in 6 M GuHCl, and monomer was isolated by gel filtration on a Superdex 75 column in 20 mM sodium phosphate buffer, pH 8, with 200 μM EDTA, and 0.02% NaN_3. The center of the monomer peak was collected on ice and lyophilized. The sample was again dissolved in 6 M GuHCl, and monomer was isolated by gel filtration on a Superdex 75 column in 20 mM sodium phosphate buffer, pH 8, with 200 μM EDTA, and 0.02% NaN_3. The gel filtration step (Figure S1) removes traces of pre-existent aggregates and exchanges the buffer to the one used in the fibril formation experiments. The peptide concentration was determined from the absorbance of the integrated peak area using ε_{280} = 1400 l mol^{-1}cm^{-1} as calibrated using quantitative amino acid analysis. The monomer generated in this way was diluted with buffer to 4 or 8 μM and supplemented with 6 μM thioflavinT (ThT) from a 1.2 mM stock. The ThT concentration, 6 μM, was chosen in a range that produces a fluorescence signal that is linearly related to the fibril concentration.[7] All samples were prepared in low-bind Eppendorff tubes (Axygen, California, USA) on ice using careful pipetting to avoid introduction of air bubbles. Each sample was then pipetted into multiple wells of a 96-well half area plate of black polystyrene with a clear bottom and PEG coating (Corning 3881, Massachusetts, USA), 100 μL per well.

Kinetic Assays. Assays were initiated by placing the 96-well plate at 37 °C under quiescent conditions in a plate reader (Fluostar Omega, Fluostar Optima or Fluostar Galaxy, BMGLabtech, Offenburg, Germany). The ThT fluorescence was measured through the bottom of the plate every 60 s with a 440 nm excitation filter and a 480 nm emission filter. The ThT fluorescence was followed for four repeats of each sample, and the whole setup was repeated twice in separate plates.

Kinetic Assays with Preformed Fibrils. The preformed fibrils for the controlled experiments with different seed concentrations (Figure 2) were prepared just prior to the trap-and-seed experiments. Kinetic experiments were set up as above for multiple samples of 4 μM Aβ42 in 20 mM sodium phosphate buffer, pH 8, with 200 μM EDTA, 6 μM ThT, and 0.02% NaN_3. The ThT fluorescence was monitored for 1.5 h to verify the formation of fibrils. The samples were then collected from the wells into low-bind tubes (Axygen, California, USA) and sonicated for 2 min in a sonicator bath at room temperature. Sonication was intended to disperse fibrils, but test experiments with preformed fibrils that were not sonicated or sonicated for 2 or 10 min in the sonicator bath gave indistinguishable results. Under the considered condition (4 μM Aβ42) the monomer concentration is negligible at equilibrium.[8] The final concentration of fibrils, in monomer equivalents, was therefore considered equal to the initial concentration of the monomer. This has been verified by ThT fluorescence, which at the working concentration of 6 μM has been proven to give a full quantitative linear response with the final fibril concentrations.[7] For the controlled experiments with different seed concentrations, the fibril concentration in each sample was then calculated from the dilution factor relying on the slow dissociation of monomers from fibrils, meaning that their concentration does not decay during the short lag time of the seeded experiment. A series of samples were prepared with twice the desired final fibril concentration, and 50 μL

dx.doi.org/10.1021/ja408765u | J. Am. Chem. Soc. 2014, 136, 219−225

was placed in each well. Fresh monomer was isolated by gel filtration as above and diluted to 8 μM in 20 mM sodium phosphate, pH 8, containing 200 μM EDTA, 6 μM ThT, 0.02% NaN_3, and 50 μL was loaded to each well using a multichannel pipet, after which the plate was placed in the plate reader, and the ThT fluorescence was monitored every 60 s under quiescent conditions at 37 °C.

Cryo- and Standard TEM. The formation of fibrils was verified using TEM. Nonseeded Aβ42 samples (4 μM Aβ42 in 20 mM sodium phosphate buffer, pH 8, with 200 μM EDTA, 6 μM ThT and 0.02% NaN_3) were incubated in 96-well plates at 37 °C in the same manner as for the aggregation kinetics experiments, and samples for electron microscopy were retrieved at different time points during the reaction. Specimens for cryo-TEM were prepared in a controlled environment vitrification system to ensure stable temperature and to avoid loss of solution during sample preparation. The specimens were prepared as thin liquid films, <300 nm thick, on lacey carbon filmed copper grids and plunged into liquid ethane at −180 °C. This leads to vitrified specimens, avoiding component segmentation and rearrangement, and water crystallization, thereby preserving original microstructures. The vitrified specimens were stored under liquid nitrogen until measured. An Oxford CT3500 cryoholder and its workstation were used to transfer the specimen into the electron microscope (Philips CM120 BioTWIN Cryo) equipped with a postcolumn energy filter (Gatan GIF100). The acceleration voltage was 120 kV. The images were recorded digitally with a CCD camera under low electron dose conditions. The same instrument was used for standard TEM. In this case a carbon-coated Formvar grid was placed upside down on a droplet of each sample followed by a quick rinse and then placing the grid upside down on a droplet of 1.5% uranyl acetate.

Trap-and-Seed Experiment. Kinetic experiments were set up as above for multiple 100 μL samples of 4 μM Aβ42 in 20 mM sodium phosphate buffer, pH 8, with 200 μM EDTA, 6 μM ThT, and 0.02% NaN_3, and the ThT fluorescence was monitored in the plate reader every 60 s at 37 °C. Every 3 min the plate was stopped, and sample from four wells was removed and centrifuged through 200 nm spin filters (Anapour) for 2 min. Fresh monomer, 100 μL of 4 μM Aβ42 in 20 mM sodium phosphate buffer, pH 8, with 200 μM EDTA, 6 μM ThT and 0.02% NaN_3) was added to each retentate in the filter unit and then placed in a well of a 96-well plate, and ThT fluorescence was recorded in the plate reader every 60 s. Each filtrate was placed in another well, and its ThT fluorescence was recorded every 60 s. The whole procedure was repeated twice. The mild sonication used in the controlled seeding for the calibration curve has no relevant impact on the fibril length distribution, and the trap-and-seed experiments were therefore performed without sonication to save handling time between the filtration and the new aggregation experiments with the retentates. In addition, in the regime of low concentration of seeds considered in the trap-and-seed experiments, secondary nucleation depending on the mass of the fibrils (and therefore independent of the length distribution) dominates over elongation events, which depend on the number of fibrils.

Theoretical Calculations of Seeded Kinetics and Scaling of the Half-Time versus Seed Concentration. In the presence of primary nucleation, elongation, depolymerization, and secondary nucleation events characterized by reaction rate constants k_n, k_+, k_{off}, and k_2, respectively, the kinetic equation governing the formation of fibril mass during time, $M(t)$, is given by:[7]

$$\frac{M(t)}{M(\infty)} = 1 - \alpha\left(\frac{B_+ + C_+}{B_+ + C_+ e^{\kappa t}}\frac{B_- + C_+ e^{\kappa t}}{B_- + C_+}\right)^{k_\infty^2/\kappa\tilde{k}_\infty} e^{-k_\infty t} \quad (4)$$

where $M(\infty)$ is the fibril mass in the long-time limit and the constants are given as

$$\alpha = 1 - \frac{M_0}{M(\infty)} \quad (5)$$

$$\kappa = \sqrt{2m_0^{n_2}(m_0k_+ - k_{off})k_2} \approx \sqrt{2m_0^{n_2+1}k_+k_2} \quad (6)$$

$$\lambda = \sqrt{2k_+k_nm_0^{n_C}} \quad (7)$$

$$C_\pm = \frac{\lambda^2}{2\kappa^2} \pm \frac{k_+P_0}{\kappa} \pm \frac{k_+M_0}{2(m_0k_+ - k_{off})} \approx \frac{\lambda^2}{2\kappa^2} \pm \frac{k_+M_0}{\kappa\bar{L}} \pm \frac{M_0}{2m_0} \quad (8)$$

$$k_\infty = \kappa\sqrt{\frac{2}{n_2(n_2+1)} + \frac{2}{n_C}\frac{\lambda^2}{\kappa^2} + \frac{2}{n_C}\frac{M_0}{m_0} + \left(\frac{2k_+P_0}{\kappa}\right)^2} \quad (9)$$

$$\tilde{k}_\infty = \sqrt{k_\infty{}^2 - 4C_+C_-\kappa^2} \quad (10)$$

$$B_\pm = \frac{\tilde{k}_\infty \pm k_\infty}{2\kappa} \quad (11)$$

m_0, M_0 and P_0 are, respectively, the monomer, the seed mass, and the seed number concentrations at time zero. The seed mass and number concentrations are connected via the average fibril length, $\bar{L} = M_0/P_0$.

■ ASSOCIATED CONTENT

Supporting Information

Materials and methods and Figures S1−S5. This material is available free of charge via the Internet at http://pubs.acs.org.

■ AUTHOR INFORMATION

Corresponding Authors

sara.linse@biochemistry.lu.se

tpjk2@cam.ac.uk

Notes

The authors declare no competing financial interest.

■ ACKNOWLEDGMENTS

The authors thank Prof. C. M. Dobson and Prof. M. Vendruscolo for helpful discussions. We thank the Crafoord Foundation (S.L.), the Swedish Research Council (S.L.), with its Linneaus Centre of Exellence Organizing Molecular Matter, the Alzheimer foundation, Sweden (S.L.), the Swiss National Science Foundation (A.P.), the BBSRC (T.P.J.K.) and the Newman foundation (T.P.J.K.), Lars Hierta Foundation (RC), Royal Fysiographic Society (R.C.), The research school FLÄK of Lund University (S.L., R.C.) for support. The expert assistance with cryo-TEM by Gunnel Karlsson, Lund University, electron microscopy unit is gratefully acknowledged.

■ REFERENCES

(1) Finder, V. H.; Glockshuber, R. *Neurodegener. Dis.* **2007**, *4*, 13.
(2) Rauk, A. *Chem. Soc. Rev.* **2009**, *38*, 2698.
(3) Swerdlow, R. H. *Neurotoxic. Res.* **2012**, *22*, 182.
(4) Serpell, L. C. *Biochim. Biophys. Acta* **2000**, *26*, 16.
(5) Jan, A.; Adolfsson, O.; Allaman, I.; Buccarello, A.-L.; Magistretti, P. J.; Pfeifer, A.; Muhs, A.; Lashuel, H. A. *J. Biol. Chem.* **2011**, *286*, 8585.
(6) Lansbury, P. T.; Lashuel, H. A. *Nature* **2006**, *443*, 774.
(7) Cohen, S. I. A.; Linse, S.; Lueshi, M. L.; Hellstrand, E.; White, D.; Rajah, L.; Otzen, D.; Vendruscolo, M.; Dobson, C.; Knowles, J. T. *Proc. Natl. Acad. Sci. U.S.A.* **2013**, *24*, 9758−9763.
(8) Hellstrand, E.; Boland, B.; Walsh, D. M.; Linse, S. *ACS Chem. Neurosci.* **2010**, *1*, 13.
(9) Linse, B.; Linse, S. *Mol. Biosyst.* **2011**, *7*, 2296.
(10) Ferrone, F. A.; Hofrichter, J.; Eaton, W. A. *J. Mol. Biol.* **1985**, *183*, 611.
(11) Lorenzen, N.; Cohen, S. I.; Nielsen, S. B.; Herling, T. W.; Christiansen, G.; Dobson, C. M.; Knowles, T. P.; Otzen, D. *Biophys. J.* **2012**, *102*, 2167.
(12) Oosawa, F.; Asakura, S. *Thermodynamics of the Polymerization of Protein*; Academic Press: London, 1975.

(13) Cohen, S. I. A.; Vendruscolo, M.; Dobson, C. M.; Knowles, T. P. J. *J. Mol. Biol.* **2012**, *421*, 160.
(14) Bartolini, M.; Bertucci, C.; Bolognesi, M. L.; Cavalli, A.; Melchiorre, C.; Andrisano, V. *ChemBioChem* **2007**, *8*, 2152.
(15) Biancalana, M.; Koide, S. *Biochim. Biophys. Acta* **2010**, *7*, 22.
(16) Saiki, R. K.; Gelfand, D. H.; Stoffel, S.; Scharf, S. J.; Higuchi, R.; Horn, G. T.; Mullis, K. B.; Erlich, H. A. *Science* **1988**, *239*, 487.
(17) Chen, B.; Morales, R.; Barria, M. A.; Soto, C. *Nat. Methods* **2010**, *7*, 519.
(18) Saborio, G. P.; Permanne, B.; Soto, C. *Nature* **2001**, *411*, 810.
(19) Du, D.; Murray, A. N.; Cohen, E.; Kim, H.-E.; Simkovsky, R.; Dillin, A.; Kelly, J. W. *Biochemistry* **2011**, *50*, 1607.
(20) Gupta, S.; Jie, S. A.; Colby, D. W. *J. Biol. Chem.* **2012**, *287*, 9982.
(21) Cox, B.; Ness, F.; Tuite, M. *Genetics* **2003**, *165*, 23.
(22) Fernandez-Bellot, E.; Cullin, C. *Cell. Mol. Life Sci.* **2001**, *58*, 1857.
(23) Walsh, D. M.; Thulin, E.; Minogue, A. M.; Gustavsson, N.; Pang, E.; Teplow, D. B.; Linse, S. *Febs J* **2009**, *276*, 1266.
(24) Cohen, S. I. A.; Vendruscolo, M.; Dobson, C. M.; Knowles, T. P. J. *J. Chem. Phys.* **2011**, *135*, 065106.
(25) Cohen, S. I. A.; Vendruscolo, M.; Welland, M. E.; Dobson, C. M.; Terentjev, E. M.; Knowles, T. P. J. *J. Chem. Phys.* **2011**, *135*, 065105.
(26) Bishop, M. F.; Ferrone, F. A. *Biophys. J.* **1984**, *46*, 631.
(27) Willander, H.; Presto, J.; Askarieh, G.; Biverstal, H.; Frohm, B.; Knight, S. D.; Johansson, J.; Linse, S. *J. Biol. Chem.* **2012**, *287*, 31608.
(28) FerroneF. *Amyloid, Prions, and Other Protein Aggregates*; Academic Press: New York, 1999, p 256; Vol. *309*.
(29) Ruschak, A. M.; Miranker, A. D. *Proc. Natl. Acad. Sci. U.S.A.* **2007**, *104*, 12341.
(30) Knowles, T. P. J.; Waudby, C. A.; Devlin, G. L.; Cohen, S. I. A.; Aguzzi, A.; Vendruscolo, M.; Terentjev, E. M.; Welland, M. E.; Dobson, C. M. *Science* **2009**, *326*, 1533.
(31) Fodera, V.; Librizzi, F.; Groenning, M.; van de Weert, M.; Leone, M. *J. Phys. Chem. B* **2008**, *112*, 3853.
(32) Ramachandran, G.; Udgaonkar, J. B. *J. Mol. Biol.* **2012**, *421*, 296.
(33) Arosio, P.; Beeg, M.; Nicoud, L.; Morbidelli, M. *Chem. Eng. Sci.* **2012**, *78*, 21.